Acta Crystallographica Section D
Biological Crystallography
ISSN 0907-4449

Crystallization and preliminary X-ray diffraction study of two complexes of a TAXI-type xylanase inhibitor with glycoside hydrolase family 11 xylanases from *Aspergillus niger* and *Bacillus subtilis*

Stefaan Sansen,[a] Camiel J. De Ranter,[a] Kurt Gebruers,[b] Kristof Brijs,[b] Christophe M. Courtin,[b] Jan A. Delcour[b] and Anja Rabijns[a]*

[a]Laboratorium voor Analytische Chemie en Medicinale Fysicochemie, Faculteit Farmaceutische Wetenschappen, K.U. Leuven, E. Van Evenstraat 4, B-3000 Leuven, Belgium, and [b]Laboratorium voor Levensmiddelenchemie, Faculteit Landbouwkundige en Toegepaste Biologische Wetenschappen, K.U. Leuven, Kasteelpark Arenberg 20, B-3001 Leuven, Belgium

Correspondence e-mail: anja.rabijns@pharm.kuleuven.ac.be

Received 27 October 2003
Accepted 18 December 2003

Endo-β-1,4-xylanases hydrolyze arabinoxylan, a major constituent of cereal cell walls, and are nowadays widely used in biotechnological processes. Purified complexes of family 11 xylanases from *Aspergillus niger* and *Bacillus subtilis* with TAXI I, a TAXI-type xylanase inhibitor from *Triticum aestivum* L., were prepared. In both cases the complex was crystallized using the hanging-drop vapour-diffusion method. The needle-like crystals of TAXI I in complex with *A. niger* xylanase belong to the trigonal space group $P3_1$ or $P3_2$, with unit-cell parameters $a = b = 88.43$, $c = 128.99$ Å, and diffract to 1.8 Å resolution. TAXI I in complex with *B. subtilis* xylanase crystallizes in the monoclinic space group $C2$, with $a = 107.89$, $b = 95.33$, $c = 66.31$ Å, $\beta = 122.24^\circ$. Complete data sets were collected for both crystal types using synchrotron radiation.

1. Introduction

Endo-β-1,4-xylanases (also referred to as endoxylanases or xylanases; EC 3.2.1.8) are classified mainly into two glycoside hydrolase families based on amino-acid sequence similarities (Henrissat, 1991; http://afmb.cnrs-mrs.fr/~cazy/CAZY/). Family 10 xylanases are characterized by a TIM-barrel $(\beta/\alpha)_8$ topology and molecular weights higher than 30 kDa, while those of family 11 are lower molecular-weight proteins of approximately 20 kDa and have a β-jelly-roll structure. Xylanases are produced by microorganisms and several plants, where they play an important role in the breakdown of the hemicellulose of cell walls. They are endo-acting and hydrolyse β-1,4-linkages between the D-xylosyl residues in xylan and arabinoxylan, releasing (arabino)xylo-oligosaccharides of different lengths (Biely *et al.*, 1997; Kulkarni *et al.*, 1999). Microbial xylanases are frequently used to modify the functionality of (arabino)xylan in feed (Bedford & Schulze, 1998) and food applications, such as breadmaking (Courtin *et al.*, 1999) and wheat gluten/starch separation (Christophersen *et al.*, 1997), and in other biotechnological processes, such as paper and pulp biobleaching (Kulkarni *et al.*, 1999).

In this context, an important recent development is the discovery of proteinaceous xylanase inhibitors in cereals such as wheat (*Triticum aestivum* L.), durum wheat (*T. durum* Desf.), barley (*Hordeum vulgare* L.) and rye (*Secale cereale* L.) (Debyser *et al.*, 1997; Debyser, 1999), which may affect the functionality of the xylanases in the above-mentioned processes and applications. To date, two distinct types of endoxylanase inhibitors have been identified in cereals: TAXI-type (*T. aestivum* xylanase inhibitor; Debyser & Delcour, 1998; Gebruers *et al.*, 2001; Goesaert *et al.*, 2001) and XIP-type (xylanase-inhibiting protein; McLauchlan *et al.*, 1999; Gebruers, Brijs *et al.* 2002; Elliott *et al.*, 2003) inhibitors. The TAXI-type inhibitors have a molecular weight of ~40 kDa and a basic pI. Some cereals, such as wheat, contain two different types of TAXI proteins, *i.e.* TAXI I-type and TAXI II-type xylanase inhibitors, which show very high sequence homology but differ from one another in pI (8.9 and at least 9.3, respectively) and xylanase specificity (Gebruers *et al.*, 2001). Both TAXI-type xylanase inhibitors specifically inhibit bacterial and fungal family 11 xylanases. While TAXI I inhibition activity does not seem to depend on the pI of the xylanases, TAXI II inhibition of family 11 enzymes with low pI values is weak or absent (Gebruers *et al.*, 2001). The XIP-type inhibitors are monomeric glycosylated proteins with pI values of 8.7–8.9 and molecular weights of 29–32 kDa (McLauchlan *et al.*, 1999; Gebruers, Brijs *et al.*, 2002; Payan *et al.*, 2003). They inhibit family 10 as well as family 11 xylanases, as long as they are of fungal origin (Flatman *et al.*, 2002). There is no sequence homology between the TAXI-type and XIP-type endoxylanase inhibitors.

Recent studies on the molecular identification, isolation and characterization of the TAXI I gene, together with screening of the available wheat EST libraries, shows that TAXI genes are expressed in different tissues

at different stages of plant development and under plant stress conditions (Fierens *et al.*, 2003). Furthermore, TAXI I shares a high sequence similarity with EDGP (extracellular dermal glycoprotein; Satoh *et al.*, 1992) and XEGIP (xyloglucan-specific endoglucanase inhibitor protein; Qiang *et al.*, 2003), both of which have been suggested to be plant defence proteins, in carrot and tomato, respectively. Hence, TAXIs belong to a newly identified class of plant proteins for which a function as plant protective microbial glycoside hydrolase inhibitors has been suggested (Fierens *et al.*, 2003).

In order to facilitate the study of the inhibitory mechanisms and the pI-dependent endoxylanase specificities of the TAXI-type endoxylanase inhibitors, a crystallographic study of TAXI I in complex with *Aspergillus niger* xylanase (pI = 3.5) and TAXI I in complex with *Bacillus subtilis* xylanase (pI = 9.3) has been undertaken. Here, we describe the crystallization and preliminary diffraction analysis of both protein–protein complexes.

2. Experimental

2.1. Purification

TAXI I was purified from wheat wholemeal (cv. Soissons) as previously described in more detail by Gebruers, Goesaert *et al.* (2002). Pure *A. niger* family 11 xylanase was obtained from Megazyme (Bray, Ireland), while *B. subtilis* family 11 xylanase was purified from the Grindamyl H 640 enzyme preparation from Danisco (Brabrand, Denmark). To this end, portions of the enzyme preparation (20.0 g) were extracted for 2 h at room temperature with 200 ml 25 m*M* sodium acetate buffer pH 4.0. The extracts were dialysed against the same buffer (18 h, 280 K) and subsequently centrifuged (10 000*g*, 30 min, 280 K). The xylanase was purified from the supernatant by cation-exchange chromatography on an SP Sepharose Fast Flow column (26 × 300 mm; Amerham Biosciences, Uppsala, Sweden) at pH 4.0 (using the same buffer) using a gradient of 0.0–0.5 *M* NaCl in 800.0 ml at a flow rate of 5.0 ml min^{-1}. 10 ml fractions were collected, screened for xylanase activity using the Xylazyme-AX method (Megazyme, Bray, Ireland) and analysed by SDS–PAGE in order to assess the purity of the enzyme. Xylanase fractions with high purity were pooled, dialysed against deionized water and finally freeze-dried.

In order to prepare the inhibitor–xylanase complexes, 4.0 mg TAXI I was incubated at room temperature for 30 min with an excess amount of *A. niger* or *B. subtilis* xylanase (20.0 mg). The inhibitor and enzyme were dissolved in 5.0 ml 25 m*M* sodium acetate buffer pH 4.5. The inhibitor–enzyme mixture was then loaded onto a MonoS HR 5/5 column (Amerham Biosciences) equilibrated with the same buffer. Elution was performed with a 0.0–0.4 *M* NaCl gradient in 30 ml at a flow rate of 1.0 ml min^{-1}. 0.5 ml fractions were collected and analyzed by SDS–PAGE. Those containing enzyme as well as inhibitor were pooled.

2.2. Crystallization and X-ray diffraction study

Prior to crystallization trials, the protein solution was further concentrated to approximately 10 mg ml^{-1} by ultrafiltration using a Microcon concentrator (Amicon) with a 3 kDa cutoff. To determine initial crystallization conditions, Hampton Research Crystal Screens I and II (Jancarik & Kim, 1991; Cudney *et al.*, 1994) were applied with hanging-drop vapour-diffusion geometry using Linbro multiwell tissue plates stored at 277 K. Each well was filled with 700 µl of reservoir solution and drops consisting of 1.5 µl protein solution and 1.5 µl of reservoir solution were placed on cover slips and set to equilibrate against these reservoir solutions. Conditions favouring crystal growth were optimized using different buffers, pH, precipitant, storage temperature and additives.

Diffraction data were collected at the ID14-1 beamline (ESRF, Grenoble) with a ADSC Q4R CCD detector. The experiments were performed at 100 K using a stream of nitrogen gas (Oxford Cryosystems Cryostream). Crystals of both inhibitor–enzyme complexes cryoprotected by soaking for 30 s in the appropriate crystallization condition to which 20% of glycerol had been added were mounted in cryoloops and flash-cooled by plunging into liquid nitrogen. All data were processed using *MOSFLM* 6.2.2 (Leslie, 1992) and *SCALA* 4.2 (Collaborative Computational Project, Number 4, 1994).

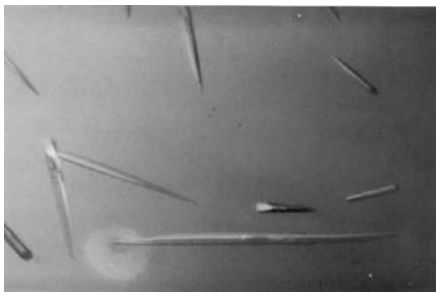

Figure 1
Needle-like crystals of TAXI I in complex with *A. niger* family 11 endoxylanase. The typical size of diffraction-quality crystals is approximately 0.8 × 0.2 × 0.2 mm.

Table 1
Data-collection and reduction statistics.

Values in parentheses are for data in the highest resolution shell.

	TAXI I–*A. niger* xylanase	TAXI I–*B. subtilis* xylanase
Space group	$P3_1$ or $P3_2$	$C2$
Wavelength (Å)	0.934	0.934
Resolution limit (Å)	1.8 (1.90–1.80)	2.50 (2.64–2.50)
Total observations	623496	51556
Unique reflections	104587 (15228)	20136 (2965)
Redundancy	5.96	2.56
Completeness		
All data (%)	100 (99.9)	98.0 (98.0)
$I > 2\sigma(I)$ (%)	89.1 (69.2)	86.7 (65.2)
$\langle I/\sigma(I)\rangle$	9.3 (4.2)	8.5 (3.8)
$R_{\rm sym}$ (%)	5.0 (17.5)	5.8 (20.1)

3. Discussion

3.1. TAXI I in complex with *A. niger* xylanase

After optimization, a solution containing 0.25 *M* magnesium acetate, 17%(*w*/*v*) polyethylene glycol 8000 and 0.1 *M* sodium cacodylate buffer pH 6.5 yielded good needle-like crystals. Crystals, as shown in Fig. 1, appeared after approximately one week. To verify whether TAXI I and *A. niger* xylanase were present, some crystals were dissolved and analyzed by SDS–PAGE. Bands corresponding to both proteins could be clearly recognized.

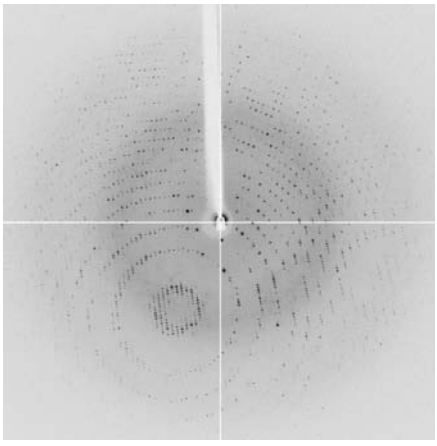

Figure 2
A typical diffraction pattern from a crystal of TAXI I in complex with *A. niger* family 11 endoxylanase obtained using 0.5° oscillation and 10 s exposure on an ADSC Q4R CCD detector at the ID14-1 beamline at the ESRF. The diffraction limit at the edge of the image was 1.8 Å.

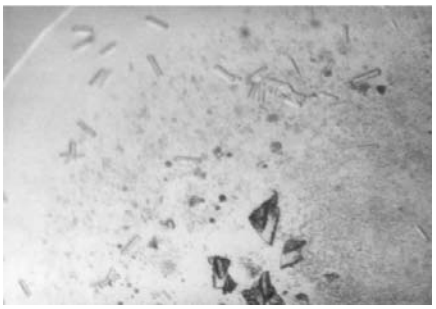

Figure 3
Small crystals of TAXI I in complex with *B. subtilis* family 11 endoxylanase.

A complete data set to a resolution of 1.8 Å was collected (Fig. 2). The space group was assigned as $P3_1$ or $P3_2$, with unit-cell parameters $a = b = 88.43$, $c = 128.99$ Å. Further statistics are summarized in Table 1. According to Matthews coefficient calculations (Matthews, 1974), the asymmetric unit should consist of two inhibitor–enzyme complex molecules, with a corresponding V_M of 2.4 Å^3 Da^{-1} and a solvent content of 48.9%. Structural analysis of this complex using the molecular-replacement method is currently in progress. To this end, the structures of TAXI I (Sansen *et al.*, 2003) and *A. niger* xylanase (PDB code 1ukr; Krengel & Dijkstra, 1996) will serve as templates in rotation and translation searches.

3.2. TAXI I in complex with *B. subtilis* xylanase

Initial crystallization trials were not successful. Only when the storage temperature was changed to 293 K did small crystals grow in mother liquor containing 25%(*w*/*v*) polyethylene glycol 4000, 0.22 *M* ammonium sulfate and 0.1 *M* sodium acetate buffer pH 4.6 (Fig. 3). The crystals reached maximum dimensions after approximately three weeks. The presence of both inhibitor and enzyme was again confirmed by SDS–PAGE analysis. A complete data set could be collected to a resolution limit of 2.5 Å (Fig. 4). Crystals belong to the monoclinic space group *C*2, with unit-cell parameters $a = 107.89$, $b = 95.33$, $c = 66.31$ Å, $\beta = 122.24^\circ$. Further statistics are summarized in Table 1. The packing density for one inhibitor–enzyme complex molecule in the asymmetric unit of these crystals is 2.6 Å^3 Da^{-1}, corresponding to an approximate solvent content of 51.7%, a reasonable value for globular proteins (Matthews, 1974). The TAXI I model, together with the *B. circulans* xylanase structure (PDB code 1c5h; Joshi *et al.*, 2001) will be used in molecular-replacement searches in order to obtain an initial model of this protein–protein complex.

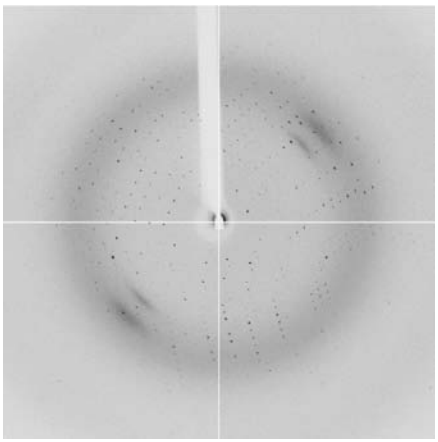

Figure 4
A typical diffraction pattern from a crystal of TAXI I in complex with *B. subtilis* family 11 endoxylanase obtained using 0.5° oscillation and 15 s exposure on an ADSC Q4R CCD detector at the ID14-1 beamline at the ESRF. The diffraction limit at the edge of the image was 2.5 Å.

AR and CMC are Postdoctoral Research Fellows of the Fund for Scientific Research-Flanders (Belgium) (FWO-Vlaanderen). Walter Jottier is acknowledged for technical assistance during in-house data collection. We acknowledge the European Synchrotron Radiation Facility and the EMBL Grenoble Outstation, in particular David Hall, for providing support for measurements at the ESRF under the European Union 'Improving Human Potential' programme. Furthermore, we gratefully acknowledge funding from the Commission of the European Communities, Specific RTD programme 'Quality of Life and Management of Living Resources', QLK1-2000-00811, 'Solving the Problem of Glycosidase Inhibitors in Food Processing'. This study does not necessarily reflect the views of the Commission and its future policy in this area. The 'Instituut voor de aanmoediging van Innovatie door Wetenschap en Technologie in Vlaanderen' (IWT-Vlaanderen) (Brussels, Belgium) is thanked for GBOU project funding.

References

Bedford, M. R. & Schulze, H. (1998). *Nutr. Res. Rev.* **11**, 91–114.
Biely, P., Vrsanská, M., Tenkanen, M. & Kluepfel, D. (1997). *J. Biotechnol.* **57**, 151–166.
Christophersen, E. A., Jacobsen, T. S. & Wagner, P. (1997). *Stärke*, **49**, 5–12.
Collaborative Computational Project, Number 4 (1994). *Acta Cryst.* D**50**, 760–763.
Courtin, C. M., Roelants, A. & Delcour, J. A. (1999). *J. Agric. Food Chem.* **47**, 1870–1877.
Cudney, B., Patel, S., Weisgraber, K., Newhouse, Y. & McPherson, A. (1994). *Acta Cryst.* D**50**, 414–423.
Debyser, W. (1999). PhD thesis. Katholieke Universiteit Leuven, Belgium.
Debyser, W. & Delcour, J. A. (1998). Patent application WO 98/49278.
Debyser, W., Derdelinckx, G. & Delcour, J. A. (1997). *J. Am. Soc. Brew. Chem.* **55**, 153–156.
Elliott, G. O., McLauchlan, W. R., Williamson, G. & Kroon, P. A. (2003). *J. Cereal Sci.* **37**, 187–194.
Fierens, K., Brijs, K., Courtin, C. M., Gebruers, K., Goesaert, H., Raedschelders, G., Robben, J., Van Campenhout, S., Volckaert, G. & Delcour, J. A. (2003). *FEBS Lett.* **540**, 259–263.
Flatman, R., McLauchlan, W. R., Juge, N., Furniss, C., Berrin, J.-G., Hughes, R., Manzanares, P., Ladbury, J. E., O'Brien, R. & Williamson, G. (2002). *Biochem. J.* **365**, 773–781.
Gebruers, K., Brijs, K., Courtin, C. M., Goesaert, H., Proost, P., Van Damme, J. & Delcour, J. A. (2002). *J. Cereal Sci.* **36**, 367–375.
Gebruers, K., Debyser, W., Goesaert, H., Proost, P., Van Damme, J. & Delcour, J. A. (2001). *Biochem. J.* **353**, 239–244.
Gebruers, K., Goesaert, H., Brijs, K., Courtin, C. M. & Delcour, J. A. (2002). *J. Enzyme Inhib. Med. Chem.* **17**, 61–68.
Goesaert, H., Debyser, W., Gebruers, K., Proost, P., Van Damme, J. & Delcour, J. A. (2001). *Cereal Chem.* **78**, 453–457.
Henrissat, B. (1991). *Biochem. J.* **280**, 309–316.
Jancarik, J. & Kim, S.-H. (1991). *J. Appl. Cryst.* **24**, 409–411.
Joshi, M. D., Sidhu, G., Pot, I., Brayer, G. D., Withers, S. G. & McIntosh, L. P. (2001). *J. Mol. Biol.* **299**, 255–279.
Krengel, U. & Dijkstra, B. W. (1996). *J. Mol. Biol.* **263**, 70–78.
Kulkarni, N., Shendye, A. & Rao, M. (1999). *FEMS Microbiol. Rev.* **23**, 411–456.
Leslie, A. G. W. (1992). *Jnt CCP4/ESF–EACMB Newsl. Protein Crystallogr.* **26**, 27–33.
McLauchlan, W. R., Garcia-Gonesa, M. T., Williamson, G., Roza, M., Ravestein, P. & Maat, J. (1999). *Biochem. J.* **338**, 441–446.
Matthews, B. W. (1974). *J. Mol. Biol.* **82**, 513–526.
Payan, F., Flatman, R., Porciero, S., Williamson, G., Juge, N. & Roussel, A. (2003). *Biochem. J.* **372**, 399–405.
Qiang, Q., Bergmann, C. W., Rose, J. K. C., Saladie, M., Kumar Kolli, V. S., Albersheim, P., Darvill, A. G. & York, W. S. (2003). *Plant J.* **34**, 327–338.
Sansen, S., Verboven, C., De Ranter, C. J., Gebruers, K., Brijs, K., Courtin, C. M., Delcour, J. A. & Rabijns, A. (2003). *Acta Cryst.* D**59**, 744–746.
Satoh, S., Sturm, A., Fujii, T. & Chrispeels, M. J. (1992). *Planta*, **188**, 432–438.